Cement & Concrete Composites 34 (2012) 1033–1043

Contents lists available at SciVerse ScienceDirect

Cement & Concrete Composites

journal homepage: www.elsevier.com/locate/cemconcomp

Development of a self-compacting gypsum-based lightweight composite

Q.L. Yu *, H.J.H. Brouwers

Department of the Built Environment, Eindhoven University of Technology, P.O. Box 513, 5600 MB Eindhoven, The Netherlands

ARTICLE INFO

Article history:
Received 25 March 2011
Received in revised form 7 May 2012
Accepted 9 May 2012
Available online 26 May 2012

Keywords:
Gypsum
Lightweight composite
Particle size distribution
Density
Mechanical properties
Thermal behavior

ABSTRACT

This article addresses experiments and theories of a self-compacting gypsum-based lightweight composite (SGLC). A β-hemihydrate is used as binder and lightweight aggregate (LWA, 0–2 mm in different size ranges) is used as aggregate into this composite. The mix of the new composite is designed based on the particle size distribution grading theory applying the modified Andreasen and Andersen (A&A) grading line [1] to obtain an optimal packing of all the used solid materials. The effect of the distribution modulus (q) in the modified Andreasen and Andersen equation is investigated. The developed mixes are studied in both fresh and hardened states, including the flowability, density, porosity, and mechanical property. The thermal behavior of the new developed composites is investigated, from its thermal physical properties, and strength degradation at elevated temperature. The study demonstrates that this new composite has significantly improved thermal and mechanical properties, compared to those of traditional gypsum plasterboard.

1. Introduction

Gypsum plaster is one of the earliest building materials elaborated by mankind and its utilization history can be traced to 4000 years ago [2]. Gypsum plasterboard is used extensively for interior walls or ceilings due to its easy fabrication features, environmental friendliness, aesthetics, low price, etc., and also especially due to its excellent fire resistance property.

Gypsum plasterboard is produced from calcium sulfate hemihydrate, which occurs in two forms, namely α- and β-type, whereas β-hemihydrate is mainly applied since the hydration product of α-hemihydrate is too brittle to be used as building material [3]. A high amount of excess water is usually needed for the β-hemihydrate hydration to produce gypsum plasterboards due to the large specific surface area of β-hemihydrate, while stoichiometrically for a full hemihydrate hydration only an initial water amount of 0.186 by mass of hemihydrate (w_0/h_0) is needed [4,5]. The removal of the excess water during the curing period leads to some conflicting consequences to the generated gypsum, such as a great consumption of heat, which is not desired and a high porosity which contributes to a good indoor thermal insulation property [4]. It was already demonstrated that a high porosity is strongly related to a low density and poor mechanical properties such as low strength, and good thermo-physical properties such as low thermal conductivity [4,6,7]. The resulted low thermal conductivity contributes to a slow heat transfer between the indoor and the outdoor environment, which leads to a better indoor thermal comfort, as well as a good fire resistance. However, a low strength causes not only a limitation of the application of gypsum boards but also very swift strength degradation during a fire, which then even leads to a quick failure of the structure it covers.

Numerous efforts have already been made to address the abovementioned problem. Fibers such as glass fiber [8,9], carbon fiber [10], polypropylene fiber [11,12], polyamide fiber [13], and polyester fiber [14] are applied extensively to reinforce the gypsum boards. These reinforcements contribute somewhat to the improvement of the gypsum plasterboard in terms of mechanical or thermal properties, but they also have certain drawbacks. Evans et al. [8] designed a lightweight glass fibers reinforced gypsum panel with a density of about 600–800 kg/m^3; however, the compressive strength of this developed panel is very low, only about 0.35 N/mm^2, which definitely limits its application. Sing and Garg [9] reported that glass fibers could not contribute to the strength improvement if shorter than 12 mm. However, for gypsum plasterboards, the normal thickness is about 12 mm, which indicates that applying longer fibers will cause mixing problems. Eve et al. [12,13] reported a reduction of both Young's modulus and strength of the gypsum composite when increasing the content of polyamide fibers and polypropylene fibers. Colak [15] investigated the methylmethacrylate polymer reinforced gypsum composites and reported that no strength improvement is achieved when the polymer content is lower than 10% by mass. Deng and Furuno [11] reported that, with a length of 12 mm and a content of 12% by mass, polypropylene fiber reinforced gypsum particleboards (gypsum as binder, and wood particles as the strengthening material) can achieve an optimal performance (physical and mechanical properties), but such a high amount of fiber reinforcement would cause a

* Corresponding author. Tel.: +31 (0)40 247 2371; fax: +31 (0)40 243 8595.
E-mail address: q.yu@bwk.tue.nl (Q.L. Yu).

0958-9465/$ - see front matter © 2012 Elsevier Ltd. All rights reserved.
http://dx.doi.org/10.1016/j.cemconcomp.2012.05.004

Nomenclature

Roman

D	particle size (μm)
h_0	initial mass of the unreacted hemihydrate (g)
m	mass (g)
q	distribution modulus
v	volume fraction
V	volume (cm^3)
w_0	initial mass of the water (g)

Greek

β_s	the water/solid percentage (vol.%) for zero slump flow condition
Γ_s	the relative slump flow of the SGLC
ρ	density (g/cm^3)
φ	volume fraction

Subscript

dh	dihydrate (gypsum)
hh	hemihydrate
i	particle size range type
lwa	lightweight aggregates
max	maximum
min	minimum
s	shrinkage
SGLC	SGLC
slwa	solid of the lightweight aggregates
w	capillary water
v	void fraction

considerable cost increase and also mixing difficulties. Hernandez-Olivares et al. [16] reported that short sisal fibers could not contribute to the fire resistance of the reinforced gypsum board.

The present research aims at the development of an environmentally friendly $CaSO_4{\cdot}H_2O$-based lightweight composite with a good fire resistance, sufficient strength, and indoor air quality improvement properties. To obtain a low thermal conductivity, a regenerated lightweight material is used into this new composite as lightweight aggregate. The particles of the lightweight material are rather closed hollow spheres, assuring a low density and a good thermal insulation. A β-hemihydrate ($CaSO_4{\cdot}0.5H_2O$) produced from flue gas desulfurization (FGD) gypsum is used here as binder. The mix of the new composite was designed based on the packing theory applying the modified Andreasen and Andersen (A&A) grading model [17] to achieve an optimal packing of all the applied solid materials. The produced composite using the mix design method was investigated from its behavior in fresh state such as flowability, and in hardened state such as density, mechanical properties like strength, and thermal physical properties such as thermal conductivity, specific heat capacity, and its fire behavior such as mass loss and strength degradation at high temperature.

2. Mix design

2.1. Grading theory

It is already well accepted that the performance of composite materials such as concrete is strongly linked to their porosity, i.e. the void fraction, which is related to the sizes and the composition of all the applied solid ingredients in the mix [18]. It was already reported that the maximum strength is attained when the porosity of a granular structure is minimal more than one century ago [19]. A minimal porosity can be theoretically achieved by an optimal particle size distribution (PSD) of all the applied solid materials in the mix, which has been addressed by researchers such as Fuller and Thompson [20] and Andreasen and Andersen [17], and given by

$$P(D) = \left(\frac{D}{D_{max}}\right)^q \quad (1)$$

where $P(D)$ is a fraction of the total solids being smaller than size D, D is the particle size (μm), D_{max} is the maximum particle size (μm), and q is the distribution modulus.

Eq. (1) is known as the Fuller curve in the case of a q of 0.5, while according to Andreasen and Andersen [17] the distribution modulus should be in the range of 1/3 to 1/2 for the densest packing. However, in this expression, the minimum particle size is not incorporated, while in reality there must be a finite lower size limit, which was considered by Funk and Dinger [1]. They proposed a modified model based on the Andreasen and Andersen Equation, which is usually called the modified Andreasen and Andersen model, reading

$$P(D) = \frac{D^q - D_{min}^q}{D_{max}^q - D_{min}^q} \quad (2)$$

where D_{min} is the minimum particle size (μm).

Applying the PSD theory, the particles can be better packed, which results in an improved hardened state properties as well as an improved workability, since more water is available to act as the lubricant between the particles [21]. In this mix design method, the modified Andreasen and Andersen curve acts as a target function for the optimization of the individual granular materials. The proportions of the individual materials in the mix design are adjusted until an optimum fit is reached between the composed mix and the target value, using an optimization algorithm as so called Least Squares Method (LSM), i.e. the deviation between target curve and composed mix expressed by the sum of the squares of the residuals (RSS) at defined particle sizes [22], as shown in Fig. 1. This is reached by employing the Solver tool in Microsoft Excel®.

The distribution modulus affects the amount of the coarse and fine particles in the mix. As reported by Hüsken and Brouwers [22], a higher distribution modulus leads to a coarser mixture while a smaller value results in a finer mixture. Hunger [23] recommended an optimal range of $0.21 < q < 0.25$ for self-compacting concrete (SCC) with the consideration of the workability. One of the objectives in the present study is the self-compacting property, i.e., the generated composite can flow freely under its own weight into any shape such as wall board or slab. Hence, the distribution modulus here will firstly also be considered using a small value applying the self-compacting concrete mix design as a reference.

As analyzed above, an optimal packing density can be obtained by applying this mix design concept. Density, however, is strongly related with thermo-physical properties such as the thermal conductivity of gypsum plasterboard [7]. Ryan [2] also reported that the thermal conductivity is proportional to the density of gypsum-based composites such as gypsum–vermiculite, gypsum–perlite, and gypsum–sand composites. Hence, the new composite developed applying this design concept will have an opposite effect, i.e. a resulted high thermal conductivity as the void content is minimized. However, a low thermal conductivity is another desired objective in the development of this new composite. This

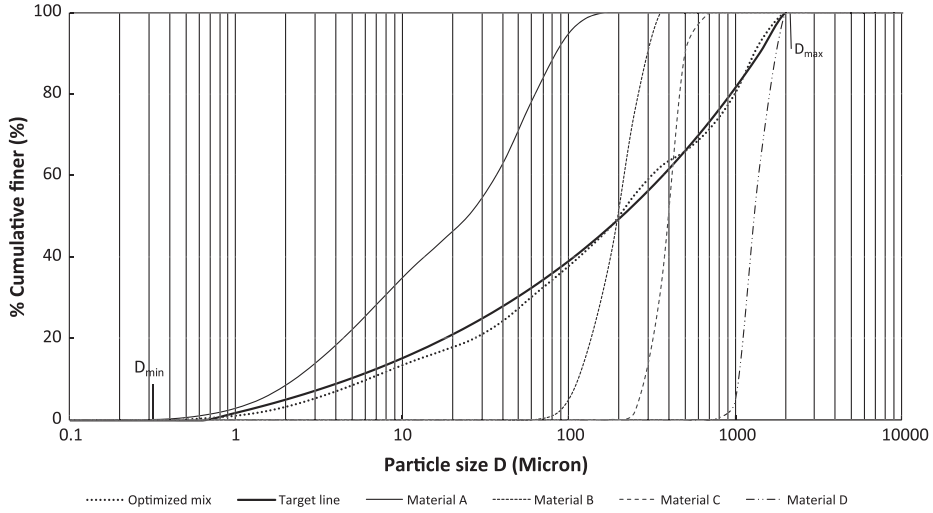

Fig. 1. PSDs of the involved ingredients, the target line and the resulting integral grading line of the mix.

paper tries to tackle this problem by applying a lightweight material as aggregate (LWA). The used LWA, made from recycled glass, are in form of closed hollow spheres, which allow a good thermal insulation property while keeping a low density. The used LWA here have size ranges of 0.1–0.3 mm, 0.25–0.5 mm, 0.5–1.0 mm, and 1.0–2.0 mm, and named LWA 0.1–0.3, LWA 0.25–0.5, LWA 0.5–1.0, LWA 1.0–2.0, respectively.

Therefore, by using β-hemihydrate as binder, the lightweight material as aggregates applying the mix design concept, the obtained self-compacting gypsum-based lightweight composite (SGLC) will have a compact structure/matrix but a large unconnected void space, which theoretically will lead to good mechanical properties as well as good thermal properties.

2.2. Mix design

As shown in Fig. 2, the volume-based composition of the developed SGLC is composed of binder (β-hemihydrate), aggregates (LWA), water (including additives such as superplasticizer) and air. Obviously the performance of the composite is related to all the ingredients. The proportions of all the solid materials are determined by the modified A&A model, whereas the distribution modulus has a significant effect. To ensure the mixed system is fluid, a thin layer of adsorbed water molecules around the particles and an extra amount of water to fill the intergranular voids of the system are necessary [24,25], as indicated in Fig. 2. The water content is strongly linked to both the flowability of the mixture in its fresh state [4,25], and the strength of the mixture in its hardened state [4]. Therefore, to design a composite with improved mechanical and thermal properties, the water content, the used solid materials, the possible admixture such as the superplasticizer will be considered simultaneously.

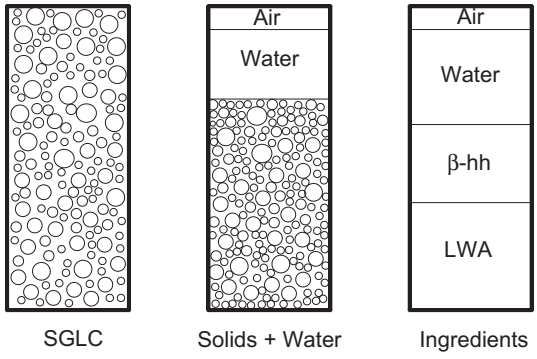

Fig. 2. Schematic diagram of the volume composition of the SGLC.

Using the self-compacting concrete mix design methodology from a guideline given by EFNARC [26] for SCC regarding specification, production and use, and Hunger [23] as reference, a mix design procedure for SGLC is derived and shown in Table 1. The first step is to collect and compute all the needed input parameters, such as the particle size distribution, the specific surface area, and the density of all the materials. The PSD of the β-hemihydrate was measured using a Mastersizer 2000, as shown in Fig. 3, with the surface weighted mean of 6.07 μm. The specific surface area was calculated from the measured PSD results based on an assumption that all the particles are spheres [27], yielding 0.377 m^2/g (9877.4 cm^2/cm^3). Here the PSDs of the LWA, measured by sieving tests, are shown in Fig. 3 as well. The chemical composition of the β-hemihydrate measured with energy-dispersive X-ray spectroscopy (EDX) is listed in Table 2, and the chemical and physical properties of the LWA taken from the data sheet from the provider are listed in Table 3, respectively.

The second step is the optimization of the proportion of all the solid materials applying the optimization algorithm. As discussed before, the distribution modulus affects greatly the designed mix proportion. Therefore here the effect of the distribution modulus on the final properties of the developed composite is studied. Applying the optimization algorithm introduced in the previous section, four mixes were developed using the same solid ingredients but different distribution moduli, which will be modified and finalized according to the desired workability.

Following the optimization of the solid ingredients, the third step is the determination of the water content, or here the water dosage based on the amount of β-hemihydrate (water/

Table 1
The description of the mix design procedure.

Design procedure	Notes
Materials characterization	Particle size distribution, specific surface area, density, etc.
Particle size distribution optimization	Mix design methodology [22,23]
Water content determination	Mini-slump flow test [4,26]
Flowability adjustment	Water content, superplasticizer [26]

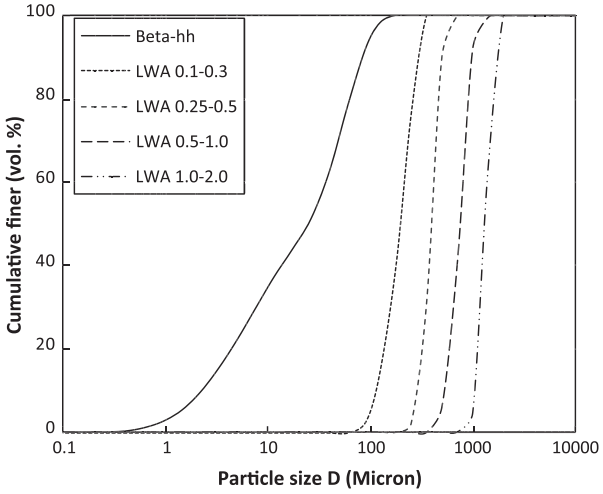

Fig. 3. The PSDs of the used solids.

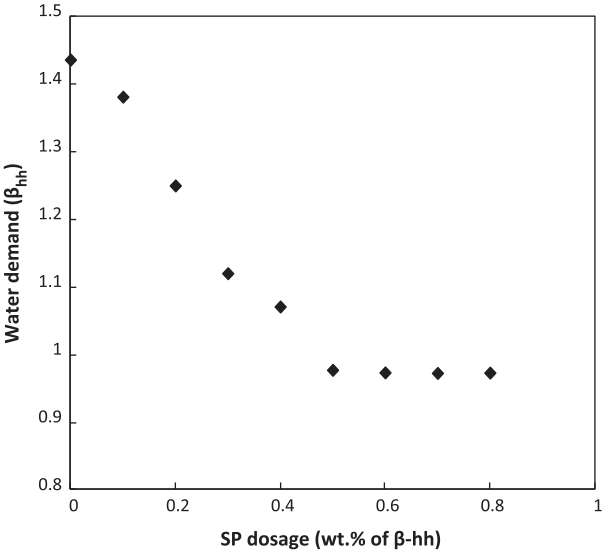

Fig. 5. The effect of the used super plasticizer on the water demand of β-hemihydrate (β_{hh}, V_w/V_{hh} at $\Gamma_{hh} = 0$).

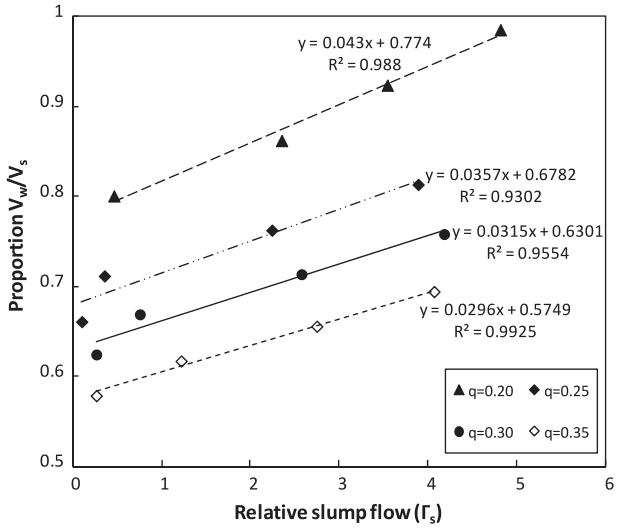

Fig. 4. V_w/V_s versus relative slump values applying the mini-slump flow test.

hemihydrate by mass). In SCC mix design, a fixed water content of about 0.30 (water/powder by mass) is usually chosen as a starting value and then adjusted according to the required flowability and viscosity [23]. Due to the obvious difference between the properties of cement and β-hemihydrate, while taking into account the LWA, this value is not suitable to be used as a reference. The water content here was first determined applying the mini-slump flow test. A Hägermann cone was deployed for the slump flow test. Firstly the slump flow of at least four mixes with the same solid proportion but different water content was tested. Then the computed relative slump flow values were plotted versus the respective water/solid volume ratio. A linear trend line was fitted through the plotted values and the water demand (β_s, which represents that in this condition the slump flow equals to zero) was derived accordingly. A detailed description of the mini-slump flow test and the calculation procedure was presented in elsewhere [4]. Fig. 4 shows the water demand results from the mix designed using different distribution moduli. It can be seen that increasing the distribution modulus resulted in a reduction of the relevant water demand although the total volume of the solids increased. This can probably be explained from the reduction of the amount of the β-hemihydrate, which also reflected the high water demand of β-hemihydrate that is in line with the previous research [4]. On the other hand, this also indicates that the water adsorption of the used lightweight aggregates within a short time (i.e. here during the spread flow test) is rather low, which is also confirmed by Liu et al. [28].

With the determined water demand, the preliminary mix design, i.e. the determination of solid materials and water content, is completed. However, it should be noted that with this water content the slump flow of the mixture is zero. The next step is to adjust the flowability of the developed mix by applying superplasticizer (SP) and slightly adjusting the water content if necessary until a desired design target. According to the standard EN 13454-2 [29], a flowable mortar and a highly plastic mortar based on gypsum should have a slump flow no less than 190 mm and 130 mm, respectively, while from EFNARC [26], the slump flow of cement mortar should be between 240 and 260 mm. Here using EFNARC [26] as a reference, the slump flow value is set as 220–250 mm. The used SP here (GPV 12), developed by SIKA [30] for the gypsum plasterboard production, is a new polycarboxylates based superplasticizer. The GPV12 is transparent solution with a specific density of 1.08 g/cm^3 and a solids content of 39.4%. Hampel [30] reported that a water reduction up to 20% is possible to get the same flow performance applying the GPV12 with an amount of 0.2% by mass of the β-hemihydrate, which is confirmed by the experimental results from the present study. Further study was carried out here to investigate the influence of GPV 12 on the water demand of the β-hemihydrate. Results are shown in Fig. 5. It is indicated that the superplasticizer has an optimal dosage amount of 0.5% by mass of the β-hemihydrate. This finding also fits to the newly developed composite from the performed

Table 2
The chemical composition of the β-hemihydrate measured with EDX.

Element	wt.%	at.%	*K*-ratio
O	48.86	67.84	0.0714
Mg	0.87	0.80	0.0030
Al	0.80	0.66	0.0037
Si	1.32	1.05	0.0082
S	21.46	14.87	0.1758
Ca	26.68	14.79	0.2285
Total	100.00	100.00	

Table 3
The chemical–physical properties of the used LWA.

Type	LWA 0.1–0.3 mm	LWA 0.25–0.5 mm	LWA 0.5–1.0 mm	LWA 1.0–2.0 mm
Physical properties				
Loose bulk density	450 ± 15 kg/m^3	300 ± 15 kg/m^3	250 ± 15 kg/m^3	220 ± 15 kg/m^3
Particle density	800 ± 15 kg/m^3	540 ± 15 kg/m^3	450 ± 15 kg/m^3	350 ± 15 kg/m^3
Crushing resistance	>3.5 N/mm^2	>2.9 N/mm^2	>2.6 N/mm^2	>2.4 N/mm^2
Chemical composition				
SiO_2	71 ± 2 wt.%	71 ± 2 wt.%	71 ± 2 wt.%	71 ± 2 wt.%
Al_2O_3	2 ± 0.3 wt.%	2 ± 0.3 wt.%	2 ± 0.3 wt.%	2 ± 0.3 wt.%
Na_2O	3 ± 1 wt.%	3 ± 1 wt.%	3 ± 1 wt.%	3 ± 1 wt.%
Fe_2O_3	0.5 ± 0.2 wt.%	0.5 ± 0.2 wt.%	0.5 ± 0.2 wt.%	0.5 ± 0.2 wt.%
CaO	8 ± 2 wt.%	8 ± 2 wt.%	8 ± 2 wt.%	8 ± 2 wt.%
MgO	2 ± 1 wt.%	2 ± 1 wt.%	2 ± 1 wt.%	2 ± 1 wt.%
K_2O	1 ± 0.2 wt.%	1 ± 0.2 wt.%	1 ± 0.2 wt.%	1 ± 0.2 wt.%
Trace	<0.5 wt.%	<0.5 wt.%	<0.5 wt.%	<0.5 wt.%

Table 4
Compositions of four mixes designed applying this mix design concept (per 1 m^3).

Material	Mix 1		Mix 2		Mix 3		Mix 4	
	Mass (kg)	Volume (m^3)	Mass (kg)	Volume (m^3)	Mass (kg)	Volume (m^3)	Mass (kg)	Volume (m^3)
β-Hemihydrate	687.0	0.262	593.8	0.227	532.6	0.203	474.0	0.181
LWA 0.1–0.3	67.9	0.084	102.9	0.127	97.5	0.121	94.8	0.117
LWA 0.25–0.5	16.9	0.031	15.8	0.029	52.5	0.097	42.1	0.078
LWA 0.5–1.0	59.4	0.132	39.6	0.088	26.3	0.058	35.1	0.078
LWA 1.0–2.0	17.0	0.049	39.6	0.113	41.3	0.118	56.2	0.160
Water	412.2	0.412	385.9	0.386	372.8	0.373	355.5	0.356
Air	0.0	0.030	0.0	0.030	0.0	0.030	0.0	0.030
SP/hemihydrate (wt./wt.)	0.20%		0.25%		0.30%		0.30%	
Water/hemihydrate (wt./wt.)	0.60		0.65		0.70		0.75	
Distribution modulus	0.20		0.25		0.30		0.35	

experiments. With the new designed composite, experimental results show that the required flowability can be reached only by adding the SP without changing the water content, as shown in Table 4.

3. Experimental

3.1. Density and porosity

As one of the objectives of this new composite development, the density and related porosity was studied at first in the present study. As shown in Fig. 2, the porosity of the developed composite is caused by three main phenomena, i.e. the chemical shrinkage during the hydration of the β-hemihydrate, the evaporation of the excess water during the curing period, and the internal open space caused by the used lightweight aggregates.

The porosity in generated gypsum formed by β-hemihydrate was already investigated [4]. An expression was proposed and validated to describe the porosity of the gypsum produced from pure β-hemihydrate, reading

$$\varphi_{v,dh} = \varphi_w + \varphi_s = \frac{\frac{w_0}{h_0} - 0.13}{\frac{\rho_w}{\rho_{hh}} + \frac{w_0}{h_0}} \tag{3}$$

where $\varphi_{v,dh}$ is volume fraction of the void in dihydrate, φ_w is volume fraction caused by the excess water, φ_s is volume fraction caused by the chemical shrinkage during the β-hemihydrate hydration, w_0/h_0 is the initial water/hemihydrate mass ratio, ρ_{hh} (g/cm^3) and ρ_w (g/cm^3) are the specific densities of hemihydrate and water, respectively.

The internal porosity of the LWA particles can be calculated from its apparent density and the specific density of the solid material, reading

$$\varphi_{v,lwa,i} = 1 - \frac{\rho_{lwa,i}}{\rho_{slwa}} \tag{4}$$

where $\varphi_{v,lwa,i}$ is porosity caused by lightweight aggregates in different size range (i), ρ_{lwa} (g/cm^3) is the apparent density of aggregate particles, and ρ_{slwa} (g/cm^3) is the specific density of the aggregate material, respectively. The density of the solid material (ρ_{slwa}) in the present study was measured using a gas Pycnometer (AccuPyc II 1340, Micromeritics) on crushed and ground samples that were obtained from ball milling method, resulting 2.458 g/cm^3 in average. The density of the aggregate particles (ρ_{lwa}) was taken from the data sheet of the provider. Hence the total porosity caused by all the LWA particles is calculated from

$$\varphi_{v,lwa} = \sum_{i=1}^{n}\left[\frac{V_{lwa,i}}{V_{SGLC}} \times \left(1 - \frac{\rho_{lwa,i}}{\rho_{slwa}}\right)\right] \tag{5}$$

where $V_{lwa,i}$ and V_{SGLC} are the volumes of the used lightweight aggregates in different size ranges i and the volume of the designed SGLC composite, respectively.

Therefore the total porosity of the new developed composite is the addition of the two parts contributed from the gypsum and the LWA separately, reading

$$\begin{aligned}\varphi_{v,SGLC} &= \varphi_{v,dh} + \varphi_{v,lwa} \\ &= \frac{\frac{w_0}{h_0} - 0.13}{\frac{\rho_w}{\rho_{hh}} + \frac{w_0}{h_0}} \times \frac{V_w + V_{hh}}{V_{SGLC}} + \sum_{i=1}^{n}\left[\frac{V_{lwa,i}}{V_{SGLC}} \times \left(1 - \frac{\rho_{lwa,i}}{\rho_{slwa}}\right)\right]\end{aligned} \tag{6}$$

where V_w and V_{hh} are the volumes of initial water content and the volume of the used β-hemihydrate amount, respectively. Incorporating the relation

$$\frac{w_0}{h_0} = \frac{\rho_w V_w}{\rho_{hh} V_{hh}} \tag{7}$$

and using $\rho_{hh}/\rho_w = 2.62$, the following expression is obtained,

$$\varphi_{v,SGLC} = 2.62 \times \left(\frac{w_0}{h_0} - 0.13\right) \times \varphi_{hh} + \sum_{i=1}^{n}\left[\varphi_{lwa,i} \times \left(1 - \frac{\rho_{lwa,i}}{\rho_{slwa}}\right)\right] \quad (8)$$

where φ_{hh} and φ_{lwa} are the volume fraction of the used β-hemihydrate and LWA in the designed composite, respectively.

It shows that the void fraction of the composite is related to the paste content (here paste is defined as the sum of water and β-hemihydrate) and the used lightweight aggregates. One can see that if the density of the LWA is the same as of the solid material, i.e. in case of the normal aggregates, Eq. (8) becomes the void fraction expression for normal gypsum board assuming the aggregates as impurities (here meaning nonreactive material).

The apparent density of the composite after removal of the free water can be calculated from the used β-hemihydrate and the aggregates, reading

$$\rho_{SGLC} = \frac{\sum_{i=1}^{n} m_{lwa,i} + 1.186 \times m_{hh}}{V_{SGLC}} \quad (9)$$

where the factor 1.186 originates from the mass of water retained by dihydrate (based on hemihydrate mass).

The derived density expression is validated by the experimental results. Here the measured density is calculated from the measured mass and size. The samples are prepared from different mix designs, whereas some of them are designed using the same distribution modulus but with different initial water content and some are designed using different distribution moduli. All the samples are cured at ambient conditions for 7 days after demolding (here demolding is performed usually 2 h after casting the samples), and then dried in a ventilated oven at 40 °C until constant mass.

The results are shown in Table 5. It is obvious that the measured density values are in excellent agreement with the calculated values, which indicates the validity of the derived density model as well as the void fraction models. Fig. 6 shows the relation between the void fraction and density and distribution modulus. The density decreases with the increase of the void fraction, which increases with the increase of the applied distribution modulus. This can be explained from Eq. (8): the increase of the distribution modulus leads to the reduction of the paste amount and to an increase of the LWA amount. Although the reduction of the paste content results in a decrease of the void fraction of the generated dihydrate, the void fraction caused by the increase of the LWA has a larger effect, which also indicates the influence of the applied distribution modulus. A further observation in Fig. 6 reveals another interesting finding, i.e. the relation between the density and the void fraction of the new composite is in line with the pure gypsum board, which was investigated in detail in [4].

The density of the newly developed composite is compared to the traditional gypsum board [4]. The comparison is carried out based on the initial water content, and the results are shown in Fig. 7. It is shown that, under all water content conditions, the density of the new composite is clearly lower than that of the traditional gypsum board; for instance, a reduction of 20% is obtained at a w_0/h_0 of 0.60. This provides a possibility to produce a much lighter building material using this mix design concept.

Table 5
The thermo–physical properties of the SGLC at room temperature.

Distribution modulus (q)	Density (g/cm^3)		Volumetric heat capacity (J/(m^3 K))
	Computed	Measured	
0.20	0.98	0.97	1.04×10^6
0.25	0.93	0.93	1.05×10^6
0.30	0.88	0.89	0.89×10^6
0.35	0.81	0.82	0.73×10^6

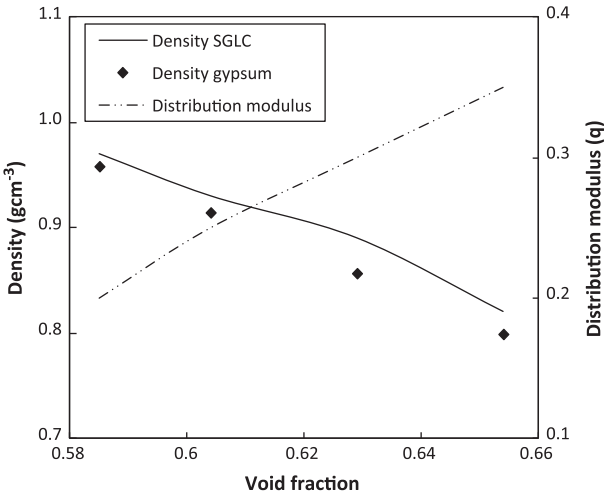

Fig. 6. The comparison of the density, void fraction and the used distribution modulus of SGLC and pure gypsum board.

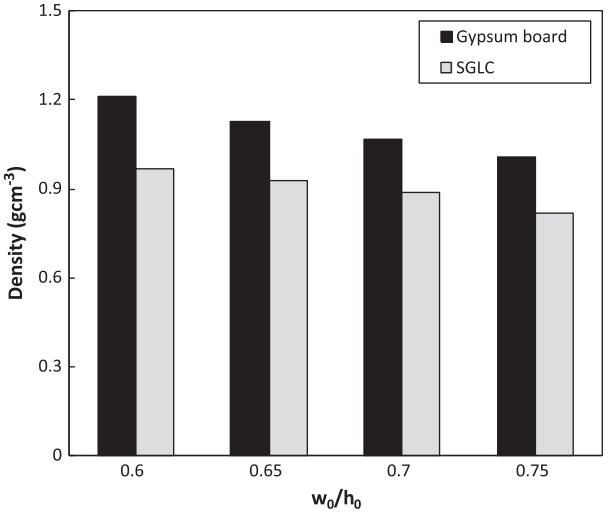

Fig. 7. The density comparison between the SGLC and pure gypsum board (data taken from [4]).

3.2. Mechanical properties

The strength development of gypsum board was already investigated previously [4]. The effect of the void fraction as well as the bonds between the gypsum crystals was analyzed and a power relation between the void fraction and strength of gypsum was found. In the present study, the mechanical properties of the new developed composite were investigated as well from its strength including the compressive and flexural strengths. Different distribution moduli lead to different mix design, while a smaller q results in a finer mixture, which obviously influences the mechanical properties such as the strength of the developed composite. In the present study, the effect of the distribution modulus was also investigated.

The flexural strength was measured on the sample with a dimension of 160 mm × 40 mm × 40 mm using the three-point bending method. The curing condition of the test samples is the same as introduced above, i.e. first they were cured at ambient

conditions for 7 days after demolding and then dried in a ventilated oven at 40 °C until the mass is constant to remove all the remaining free water. The size of the sample was strictly controlled to assure a representative value since according to Coquard et al. [31] that the sample size has an obvious influence on the measured strength. A load was applied vertically by means of a loading roller to the opposite side face of the prism with a rate of (50 ± 10) N/s until fracture. The compressive strength was measured with the half prisms left from the flexural strength test on the molded side faces over an area of 40 mm × 40 mm. A load was applied and increased smoothly at the rate of (2400 ± 200) N/s over the entire load application until fracture. The flexural and compressive strength are calculated according to the expressions given in EN 13279-2:2004 [32].

The measured compressive and flexural strength are shown in Fig. 8a and b, respectively. Both the compressive and the flexural strength decrease with the increase of the distribution modulus (q), but the strengths are influenced more significantly at a bigger q range. The compressive strength decreases only with 3.6% when the q increases from 0.20 to 0.25, but it decreases with 18.5% when the q increases to 0.30, while the related flexural strength decrease is 8.8% and 32.2%, respectively. This finding indicates from the point of view of strength that a smaller q is more suitable and recommended.

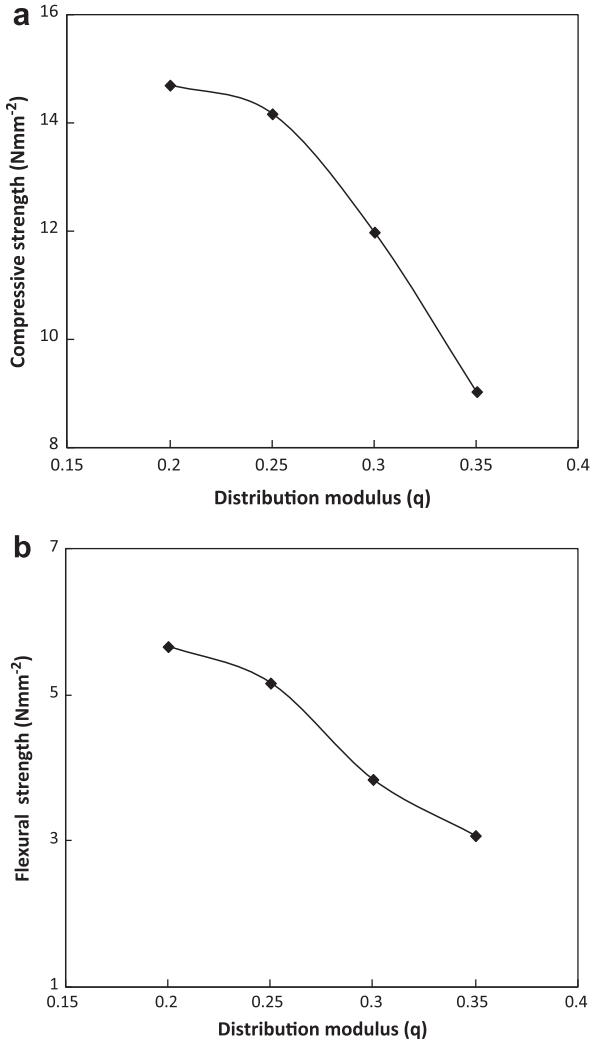

Fig. 8. The strength versus the distribution modulus ((a) compressive strength; (b) flexural strength).

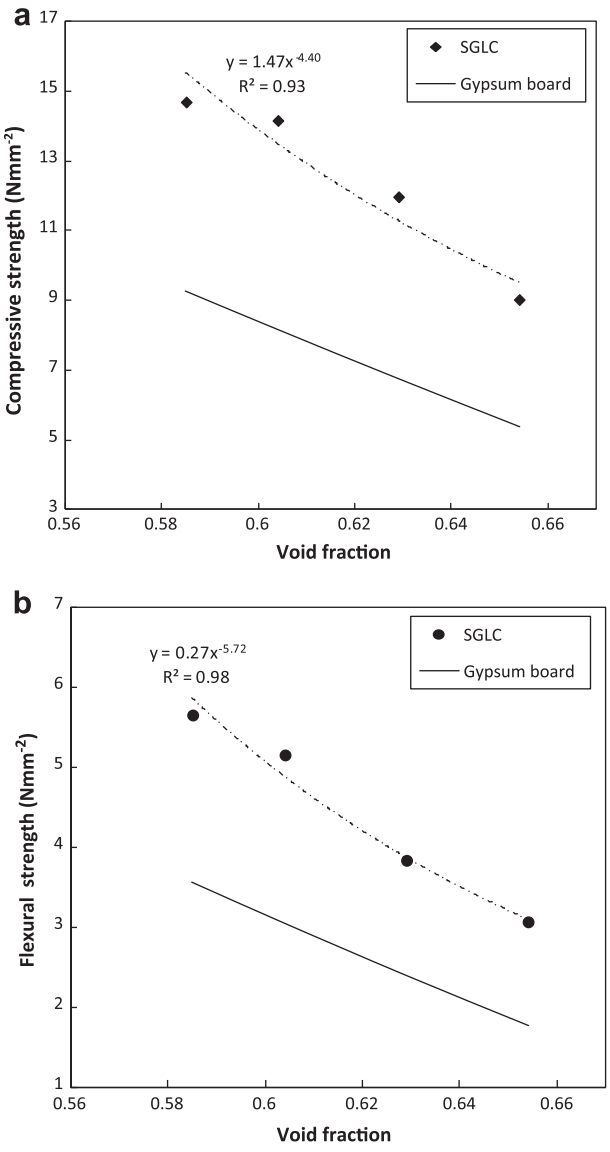

Fig. 9. The strength comparison of the new composite and pure gypsum board versus the computed void fraction ((a) compressive strength; (b) flexural strength).

The relation between the void fraction and the strength is plotted in Fig. 9. It is shown that the strength (both the compressive and flexural strength) has a power law relation with the void fraction. This is in line with the finding of the void fraction and the strength of pure gypsum [4]. The comparison of the strength between the new developed composite and pure gypsum board is also shown in Fig. 9. Here the strength value for pure gypsum board was taken from the power model derived from the previous study [4]. It can be seen, for instance with a void fraction of 0.60, the new developed composite (designed with the distribution modulus of 0.25, and it has a similar density as the traditional gypsum board of 0.93 g/cm^3), an improvement of 73.3% and 70.0% in compressive and flexural strength respectively was obtained. Hence it is demonstrated here that, a much higher strength can be reached while keeping a similar density/porosity in this new developed composite.

3.3. Thermal properties

As one of the key topics in building research, fire resistance is always receiving special attention due to the very important role

it plays in the safety of human beings. To prevent the premature collapse when heated, the main building structures should have good fire separations. To ensure an excellent fire resistance of a building structure, good thermo-physical properties such as a low thermal conductivity are very important to be obtained. On the other hand, a low thermal conductivity of the applied building structure also contributes to a good thermal comfort, due to the low heat transfer through it between the indoor and outdoor conditions.

Specific heat capacity is the measure of the heat energy required to increase the temperature of a unit quantity of a substance by a certain temperature interval, while the thermal conductivity is the property of a material that indicates its ability to conduct heat. Hence both properties are very important to obtain a good fire safety as well as a higher indoor thermal comfort. The thermal conductivity of one material is related with its density and composition, which was already extensively studied [7,33–35]. In the present study, the thermal conductivity and the volumetric specific heat capacity of the newly developed SGLC were investigated.

A commercial heat transfer analyzer (ISOMET Model 2104) was deployed here. It applies a dynamic measurement method to determine simultaneously the volumetric heat capacity (J/(m^3 K^1)) and the thermal conductivity (W/(m K)) of a material with a measurement time about 8–16 min [36]. For the measurement, a sample was produced with a unified size of 200 mm × 100 mm × 30 mm, and the sample was always first cured at ambient conditions for 7 days after demolding, and then was dried in a ventilated oven at 40 °C until the mass is constant.

The measured thermal conductivity versus the applied distribution modulus is shown in Fig. 10a. The thermal conductivity first decreases and then remains stable with the increase of the distribution modulus, whereas a minimum value of 0.19 W/(m K) is reached at a distribution modulus of 0.30. Fig. 10b shows the relation between the densities of the composites and their thermal conductivities. It is shown that the thermal conductivity remains stable at a lower density and then increases quickly with the increase of the density. This is in line with De Korte and Brouwers [33] and Zehner and Schlunder [34], who reported that the thermal conductivity is related not only with the density, but also strongly with the composition. It should also be pointed out that, to reach a lower thermal conductivity, it is not enough only to consider the reduction of the density. Here, a thermal conductivity of 0.21 W/(m K) is obtained at a void fraction of 0.60 (with the density of 0.93 g/cm^3), while in the previous section a thermal conductivity of 0.30 W/(m K) is obtained at the same void fraction for pure gypsum board [7]. Hence, it can be concluded that a 30% improvement of the thermal conductivity is reached with the SGLC.

The measured volumetric specific heat capacity is listed in Table 5. It can be noticed that the density is again not linked linearly with the volumetric specific heat capacity, and an optimal value was obtained at the distribution modulus of 0.25. Compared to the normal gypsum board, the volumetric specific heat capacity of the new SGLC is slightly lower at a same void fraction (density), for instance, the volumetric specific heat capacity is 1.05 × 10^6 J/(m^3 K) with a density of 0.93 g/cm^3, whereas it is 1.20 × 10^6 J/(m^3 K) with a similar density (0.96 g/cm^3) in the case of normal gypsum board. This probably can be explained from the difference between the composition of normal gypsum board and the developed SGLC, especially the applied LWA inside.

3.4. Thermal degradation at high temperature

When exposed to fire or under high temperature, the chemically combined water in gypsum ($CaSO_4{\cdot}2H_2O$) dissociates from the crystal lattice and vaporizes, which is known as dehydration, reading

$$CaSO_4 \times 2H_2O + \text{heat} \rightarrow CaSO_4 \times \frac{1}{2}H_2O + \frac{3}{2}H_2O \quad (10)$$

$$CaSO_4 \times \frac{1}{2}H_2O + \text{heat} \rightarrow CaSO_4 + \frac{1}{2}H_2O \quad (11)$$

During this process, gypsum absorbs a large amount of heat that drastically delays the process of heat transfer through the plasterboard [7], which is also the reason why gypsum boards are usually used as fire retardants to protect components of wall assemblies from overheating. As shown in Eqs. 10, 11, the change of the mass upon the dehydration of gypsum was caused by the release of the chemically combined water, because the used LWA is made of glass, which will not lose any weight in this temperature range. Therefore, the density of the composite at high temperature (here emphasis is focused on the dehydration temperature of dihydrate) can be theoretically calculated using the same method as discussed in the previous section given a known mixture, reading

$$\rho_{SGLC,220} = \frac{\sum_{i=1}^{n} m_{lwa,i} + 0.938 \times m_{hh}}{V_{SGLC}} \quad (12)$$

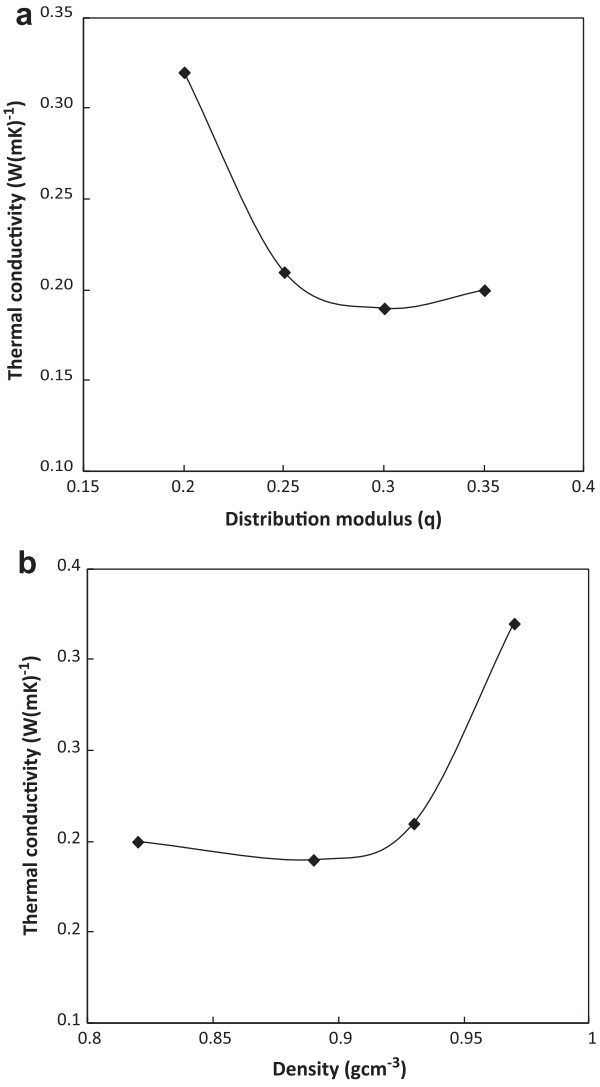

Fig. 10. The measured thermal conductivity ((a) versus the used distribution modulus; (b) versus the density).

where the factor 0.938 originates from the water release during the dehydration of dihydrate to anhydrite (as shown in Eqs. 10, 11).

However, as reported in our pervious study [7], due to the dehydration reaction, the matrix in the gypsum is changed, which results in a reduced mechanical property, e.g. strength. In the present study, lightweight material was used as aggregates, and due to the stability of its microstructure at the dehydration temperature of the gypsum, i.e. below 300 °C [7]. It will contribute to reduce the thermal degradation of the developed composite, i.e. the thermal mass loss and the strength reduction beyond the gypsum dehydration. Both the thermal mass loss and strength degradation test were carried out on the samples with a size of 160 mm × 40 mm × 40 mm. The strength (both the compressive and flexural strengths) test was done using the same procedure as introduced in the previous section. The dehydration experiments were performed following this procedure, i.e. firstly the samples were cured at ambient conditions for 7 days after demolding, and then were heated at 220 °C until the mass is constant. According to our previous study [7], this temperature assures a full dehydration reaction of gypsum given sufficient time.

Table 6
The thermo–physical properties of the SGLC after the gypsum dehydrated to anhydrite.

Distribution modulus (q)	Density (g/cm^3)		Thermal conductivity (W/(m K))	Volumetric heat capacity (J/(m^3 K))
	Computed	Measured		
0.20	0.81	0.80	0.15	0.62×10^6
0.25	0.75	0.78	0.13	0.63×10^6
0.30	0.74	0.74	0.12	0.55×10^6
0.35	0.71	0.69	0.12	0.54×10^6

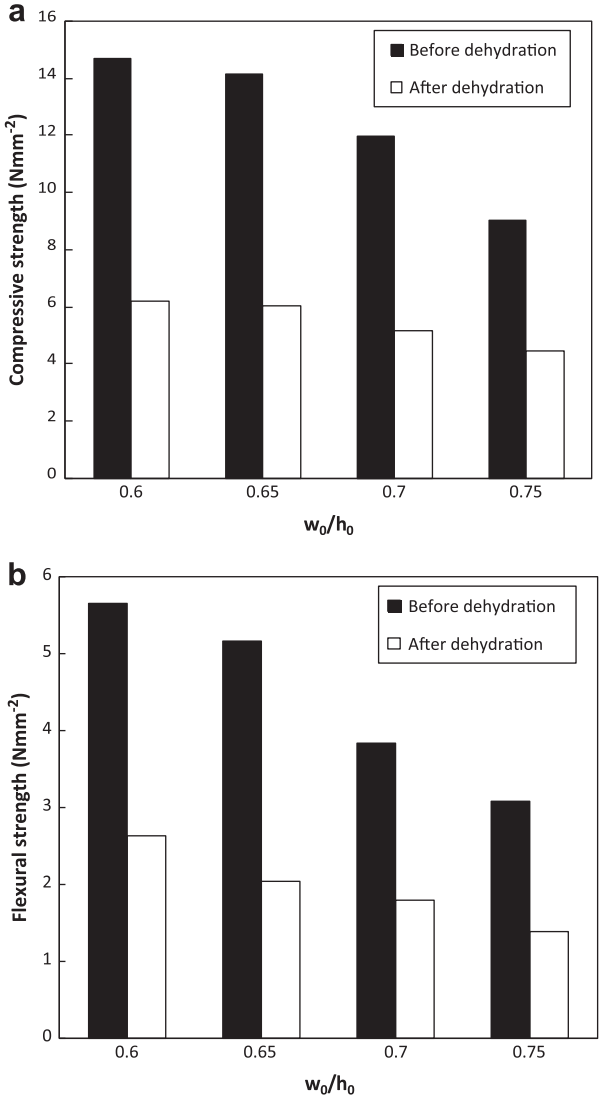

Fig. 11. The strength reduction after the gypsum in the SGLC is dehydrated to anhydrite ((a) compressive strength; (b) flexural strength).

The measured and the theoretical mass loss due to the dehydration of the gypsum at high temperature are listed in Table 6. It can be seen that the measured values are in good agreement with the computed values. The thermal mass loss leads to the microstructure change of the gypsum in the matrix of the composite, as reported in the previous study [7]: the regular gypsum crystals changed to irregular broken anhydrite particles, which resulted in a weaker bonding between the particles. The measured thermal conductivity and the volumetric specific heat capacity of the composite after dehydration are also listed in Table 6. It is obvious that the thermal conductivity became smaller after the gypsum dehydration due to the extra void caused by the release of the chemically combined water in gypsum, as well as the change of the matrix. Moreover, it is clear that the thermal conductivity of the dehydrated composite has the similar feature as the composite before dehydration, i.e. it decreased and then reached to a stable condition within the investigated distribution modulus range.

The measured strength values (both the compressive and flexural strength) are shown in Fig. 11. It can be noticed that a reduction of about 50% in both compressive and flexural strength occurred after the dehydration of gypsum, i.e. the binder in the matrix. However, compared to the current composite the pure gypsum board loses more than 80% of its strength at this temperature range [7]. Hence, one can see that, although there is obvious strength degradation, a considerable improvement has already reached in the new composite. Once again the improvement obtained here can be explained by the application of the LWA. This improvement can definitely help to delay the failure of the structure itself, and then even the whole building structure it protects.

4. Discussion

Distancing from traditional methods to reinforce gypsum boards, the present paper aims to develop a type of novel lightweight composite using β-hemihydrate as binder with an improved performance to be used as indoor wall board, fire separation structures, ceiling, etc. The modified A&A grading curve has already been applied extensively for concrete mix design, while here it is applied to design this composite with β-hemihydrate as binder instead of cement. To the authors' knowledge, this has never been reported before. Depending on the desired performance, different distribution moduli were recommended for the concrete mix design [22,23,25,37]. As a binder, hemihydrate behaves very differently from cement, therefore the effect of the distribution modulus is investigated as well.

The experiments are performed focusing on the targeted objectives: low density, good mechanical properties, and good thermal properties (e.g. low thermal conductivity). As indicated by the results presented in the previous sections, the distribution modulus indeed influences the designed composite significantly. As indicated from Fig. 6, increasing the distribution modulus leads to a reduction of the density of the composite. Hence, it seems wise to use a larger distribution modulus if we only consider the density as the key factor. However, as shown in Fig. 8, an increase of the distribution modulus results in a swift decrease of both the

compressive and flexural strength of the composite. Thus, a smaller value of q should be considered if only strength is the target value. Therefore, taking both density and strength into account, one already can see that an intermediate value of q should be used. Then, considering a thermo-physical property such as thermal conductivity, as shown in Fig. 10a, it is obvious that we should not use the smallest distribution modulus investigated here, since at that value the composite has the highest thermal conductivity. So taking all these three factors into consideration, it is already clear that a distribution modulus of 0.25 provides optimal results.

The question then rises here, whether it is useful to apply this mix design method for the calcium sulfate-based composite design when we have already found an optimal value for the distribution modulus. This can be answered from the comparison of strength, density, and thermal conductivity between the currently developed composite and the normal or traditional gypsum board, as shown in Figs. 7 and 9, as well as in Fig. 11. The significant improvement of all the investigated properties clearly indicates that this mix design method works not only for concrete mix design but also for this calcium sulfate-based composite design.

It is different from concrete design where some constraints usually have to be considered from the point of relevant regulations or practical situation. In the present study all the considerations are only taken from the point of view of the performance of the designed composite. For instance, in concrete design the used cement content should not reach a minimum or maximum given value. Here, a relatively large amount of β-hemihydrate as binder is used; on one hand it provides more binder as well as fine powders to ensure a good viscosity to resist the floating of the applied lightweight aggregates in fresh state, and on the other hand it helps to reduce the cost of the composite.

5. Conclusions

This article addresses the development of a self-compacting gypsum-based lightweight composite. The modified Andreasen and Andersen grading line was used to design the composite with an optimal packing property. β-hemihydrate was used as binder and one type of lightweight material was used as aggregates in this composite. The following conclusions are drawn:

1. A mix design methodology originally for concrete design is presented and applied to design the calcium sulfate-based lightweight composite. The mix design applies the geometric packing theory as the basic principle and the effect of the parameters in the mix design model is discussed; several mixes of the composite designed using different distribution moduli are presented. An optimal distribution modulus of 0.25 in the modified A&A equation was found to reach an optimal thermal and mechanical properties of this composite.
2. The density as well as the void fraction of the developed composite in its hardened state is studied by both modeling and experiments; a relation between the void fraction and the density is reported.
3. The mechanical properties of the developed composite are investigated. The strengths of the SGLC are compared to the traditional gypsum plasterboard, and the significant improvement, up to 70% with the same void fraction, indicates the validity of the applied mix design method.
4. The thermo-physical properties of the new composite are investigated and a 30% improvement compared to that of traditional gypsum plasterboard is reached with the same density.
5. The thermal degradation of the designed samples beyond the dihydrate dehydration temperature is studied, and a reduction of about 50% while a reduction of more than 80% in strength is found in the developed SGLC and traditional gypsum board, respectively. The comparison between the developed SGLC and traditional gypsum plasterboards from both the thermo-physical properties and the thermal degradation behavior indicates the superiority of the developed SGLC.

Acknowledgements

The authors wish to express their appreciations to Prof. H. Hummel and Mrs. K. Engelhardt from Knauf Gips KG (Germany) for gypsum related material supply, and Dr. Ch. Hampel from Sika Technology AG (Switzerland) for the superplasticizer supply. They furthermore express their gratitude to the European Commission (I-SSB Project, Proposal No. 026661-2) for funding this research, as well as to the following sponsors: Bouwdienst Rijkswaterstaat, Graniet-Import Benelux, Kijlstra Betonmortel, Struyk Verwo, Attero, Enci, Provincie Overijssel, Rijkswaterstaat Directie Zeeland, A&G Maasvlakte, BTE, Alvon Bouwsystemen, V.d. Bosch Beton, Selor, Twee "R" Recycling, GMB, Schenk Concrete Consultancy, Intron, Geochem Research, Icopal, BN International, APP All Remove, Consensor, Eltomation, Hess ACC Systems, and Kronos International (chronological order of joining).

References

[1] Funk JE, Dinger DR. Predictive process control of crowded particulate suspensions, applied to ceramic manufacturing. Boston, the United States: Kluwer Academic Publishers; 1994.
[2] Ryan JV. Study of gypsum plasters exposed to fire. J Res Natl Bureau Standards C Eng Instrum 1962;66C(4):373–87.
[3] Wirsching F. Calcium sulfate. Weinheim: Wiley-VCH Verlag GmbH & Co. KGaA; 2005.
[4] Yu QL, Brouwers HJH. Microstructure and mechanical properties of β-hemihydrate produced gypsum: an insight from its hydration process. Constr Build Mater 2011;25:3149–57.
[5] Yu QL, Brouwers HJH, De Korte ACJ. Gypsum hydration: a theoretical and experimental study. In: Fischer HB, editor. Proceedings of 17th international conference in building materials (Internationale Baustofftagung), vol. 1. Weimar: Germany; 2009. p. 783–8.
[6] Schiller KK. Strength of highly porous brittle materials. Nature 1957;180:862–3.
[7] Yu QL, Brouwers HJH. Thermal properties and microstructure of gypsum board and its dehydration products: a theoretical and experimental investigation. Fire Mater, in press. http://dx.doi.org/10.1002/fam.1117.
[8] Evans TJ, Majumdar AJ, Ryder JF. A semi-dry method for the production of lightweight glass–fibre-reinforced gypsum. Int J Cem Compos Lightweight Concr 1981;3(1):41–4.
[9] Sing M, Garg M. Glass fiber reinforced water-resistant gypsum-based composites. Cem Concr Compos 1992;12(1):23–32.
[10] Tagge CD, Pollock JF, Torres L, Soane DS. Reinforced wallboard. United States Patent 6841232; 2005.
[11] Deng YH, Furuno T. Study on gypsum-bonded particleboard reinforced with polypropylene fibers. Jpn Wood Res Soc 2001;47:445–50.
[12] Eve S, Gomina M, Orange G. Effects of polyamide and polypropylene fibers on the setting and the mechanical properties of plaster. Key Eng Mater 2004;264–268:2531–6.
[13] Eve S, Gomina M, Hamel J, Orange G. Investigation of the setting of polyamide fibre/latex-filled plaster composites. J Eur Ceram Soc 2007;27:3517–25.
[14] Dweck J, Mladenovic A, Suput JS. Thermal characterization of polymeric plaster composites. J Therm Anal Calorim 2002;67:321–6.
[15] Colak A. Physical and mechanical properties of polymer–plaster composites. Cem Concr Res 2001;31(11):1539–47.
[16] Hernandez-Olivares F, Oterza I, Villanueva LD. Experimental analysis of toughness and modulus of rupture increase of sisal short fibre reinforced hemihydrated gypsum. Compos Struct 1992;22:123–37.
[17] Andreasen AHM, Andersen J. Über die Beziehungen zwischen Kornabstufungen und Zwischenraum in Produkten aus losen Körnern (mit einigen Experimenten). Kolloid-Zeitschrift 1930;50:217–28 [in German].
[18] Brouwers HJH. A hydration model of Portland cement using the work of Powers and Brownyard. Eindhoven University of Technology & Portland Cement Association; 2011.
[19] Feret R. Sur la compactié des mortiers hyrdauliques. Ann Ponts Chauss 1892;7(IV):5–16 [in French].
[20] Fuller WB, Thompson SE. The laws of proportioning concrete. Trans Am Soc Civil Eng 1907;33:222–98.
[21] Hunger M, Brouwers HJH. Natural stone waste powders applied to SCC mix design. Restor Build Monum 2008;14:131–40.

[22] Hüsken G, Brouwers HJH. A new mix design concept for earth-moist concrete: a theoretical and experimental study. Cem Concr Res 2008;38:1246–59.
[23] Hunger M. An integral design concept for ecological self-compacting concrete. PhD thesis. Eindhoven: Eindhoven University of Technology; 2010.
[24] Hunger M, Brouwers HJH. Flow analysis of water–powder mixtures: application to specific surface area and shape factor. Cem Concr Compos 2009;31:39–59.
[25] Fennis SAAM. Design of ecological concrete by particle packing optimization. PhD thesis. Delft: Delft University of Technology; 2011.
[26] EFNARC. The European guidelines for self-compacting concrete specification, production and use. EFNARC; 2005.
[27] Mastersizer 2000, user manual. Malvern Instruments Ltd.; 2007. p. 73–4.
[28] Liu X, Chia KS, Zhang MH. Development of lightweight concrete with high resistance to water and chloride-ion penetration. Cem Concr Compos 2010;32:757–66.
[29] EN 13454-2. Binders, composite binders and factory made mixtures for floor screeds based on calcium sulfate – Part 2: test methods; 2004.
[30] Hampel C. Polymer 1* or 2* produced in full production scale (about 3 tons) for extended production tests of gypsum plasterboards. EU Project I-SSB report; 2010.
[31] Coquard P, Boistelle R, Amathieu L, Barriac P. Hardness, elasticity modulus and flexion strength of dry set plaster. J Mater Sci 1994;29:4611–7.
[32] EN 13279-2. European Standard. Gypsum binders and gypsum plasters. CEN; 2004.
[33] De Korte ACJ, Brouwers HJH. Calculation of thermal conductivity of gypsum plasterboards at ambient and elevated temperature. Fire Mater 2010;34:55–75.
[34] Zehner P, Schlunder EU. Thermal conductivity of granular materials at moderate temperatures. Chem Ing Tech 1970;42(14):933–41.
[35] Somerton WH, Chu SL, Keese JA. Thermal behavior of unconsolidated oil sands. Soc Petrol Eng AIME J 1974;14(5):513–21.
[36] ISOMET. ISOMET Model 2104 manual; 2009.
[37] Villar J, Baret JF. Cementing slurry and method of designing a formulation. Patent 6153562; 1997.